### Title

Effect of Stratification on Surface Properties of Corneal Epithelial Cells.




### Journal

Investigative ophthalmology & visual science, 56(13)

### ISSN

0146-0404



### Authors

Yáñez-Soto, Bernardo
Leonard, Brian C
Raghunathan, Vijay Krishna
et al.



### Publication Date

2015-12-01

### DOI

10.1167/iovs.15-17468

Peer reviewed

# Effect of Stratification on Surface Properties of Corneal Epithelial Cells

Bernardo Yáñez-Soto,[1–3] Brian C. Leonard,[4] Vijay Krishna Raghunathan,[2] Nicholas L. Abbott,[3] and Christopher J. Murphy[2,5]

[1]Instituto de Física Manuel Sandoval Vallarta, Universidad Autónoma de San Luis Potosí, San Luis Potosí, San Luis Potosí, México
[2]Department of Veterinary Surgical and Radiological Sciences, School of Veterinary Medicine, University of California Davis, Davis, California, United States
[3]Department of Chemical and Biological Engineering, School of Engineering, University of Wisconsin-Madison, Madison, Wisconsin, United States
[4]William R. Pritchard Veterinary Medical Teaching Hospital, School of Veterinary Medicine, University of California Davis, Davis, California, United States
[5]Department of Ophthalmology and Vision Science, School of Medicine, University of California Davis, Davis, California, United States

Correspondence: Nicholas L. Abbott, 3016 Engineering Hall, 1415 Engineering Drive, Madison, WI 53706, USA;
abbott@engr.wisc.edu.
Christopher J. Murphy, 1423 Tupper Hall, University of California Davis, 1 Shields Avenue, Davis, CA 95616, USA;
cjmurphy@ucdavis.edu.

BYS and BCL contributed equally to this work and should therefore be regarded as equivalent authors.

Submitted: June 11, 2015
Accepted: October 13, 2015

Citation: Yáñez-Soto B, Leonard BC, Raghunathan VK, et al. Effect of stratification on the surface properties of corneal epithelial cells. *Invest Ophthalmol Vis Sci*. 2015;56:8340–8348. DOI:10.1167/iovs.15-17468

**Purpose.** The purpose of this study was to determine the influence of mucin expression in an immortalized human corneal epithelial cell line (hTCEpi) on the surface properties of cells, such as wettability, contact angle, and surface heterogeneity.

**Methods.** hTCEpi cells were cultured to confluence in serum-free medium. The medium was then replaced by stratification medium to induce mucin biosynthesis. The mucin expression profile was analyzed using quantitative PCR and Western blotting. Contact angles were measured using a two-immiscible liquid method, and contact angle hysteresis was evaluated by tilting the apparatus and recording advancing and receding contact angles. The spatial distribution of mucins was evaluated with fluorescently labeled lectin.

**Results.** hTCEpi cells expressed the three main ocular mucins (MUC1, MUC4, and MUC16) with a maximum between days 1 and 3 of the stratification process. Upon stratification, cells caused a very significant increase in contact angle hysteresis, suggesting the development of spatially discrete and heterogeneously distributed surface features, defined by topography and/or chemical functionality. Although atomic force microscopy measurements showed no formation of appreciable topographic features on the surface of the cells, we observed a significant increase in surface chemical heterogeneity.

**Conclusions.** The surface chemical heterogeneity of the corneal epithelium may influence the dynamic behavior of tear film by "pinning" the contact line between the cellular surface and aqueous tear film. Engineering the surface properties of corneal epithelium could potentially lead to novel treatments in dry eye disease.

Keywords: dry eye, mucins, surface heterogeneity, surface phenomena

Dry eye syndrome is a multifactorial disease of the ocular surface, with clinical findings that include discomfort, visual disturbance, and tear film instability.[1] In the United States, it is estimated that 7.8% of women 50 years of age and older[2] and 4.34% of men 50 years of age and older[3] are affected by dry eye syndrome. Although the International Dry Eye Workshop categorized the types of dry eye as (1) aqueous-deficient and (2) evaporative,[1] dry eye syndrome and other ocular surface disorders also involve the interaction between the cellular surface of the eye and the liquid film constituted by the tears.[4]

It is widely believed that the stability/instability of tear film depends on the surface properties of the epithelium, especially its wettability or degree of retention of tear film in contact with the ocular surface.[5–7] Although wetting properties have conventionally been attributed to the presence of a hydrophilic glycocalyx,[8] specifically to the highly O-glycosylated membrane-associated mucins of the ocular surface (principally MUC1, MUC4, and MUC16),[9] to our knowledge, there are no studies that directly correlate the expression and spatial distribution of cell associated mucins to the physicochemical surface properties of the ocular surface.

Immortalized corneal epithelial cell lines have been reported to differentiate, stratify, and express significant amounts of mucins when cultured as a confluent monolayer of cells and stimulated with 10% fetal bovine serum and 10 ng/mL epithelial growth factor (EGF).[10] In this work we induced stratification of an hTERT immortalized corneal epithelial (hTCEpi) cell line[11] over a period of 6 days and characterized the expression of mucins to correlate with the surface properties of the cells.

A standard method to evaluate surface properties is the sessile drop contact angle technique.[5–7,12] This widely used method is performed by measuring the contact angle between a drop of liquid and a solid in air. However, measurements of the contact angle of water drops on cell cultures or tissues are

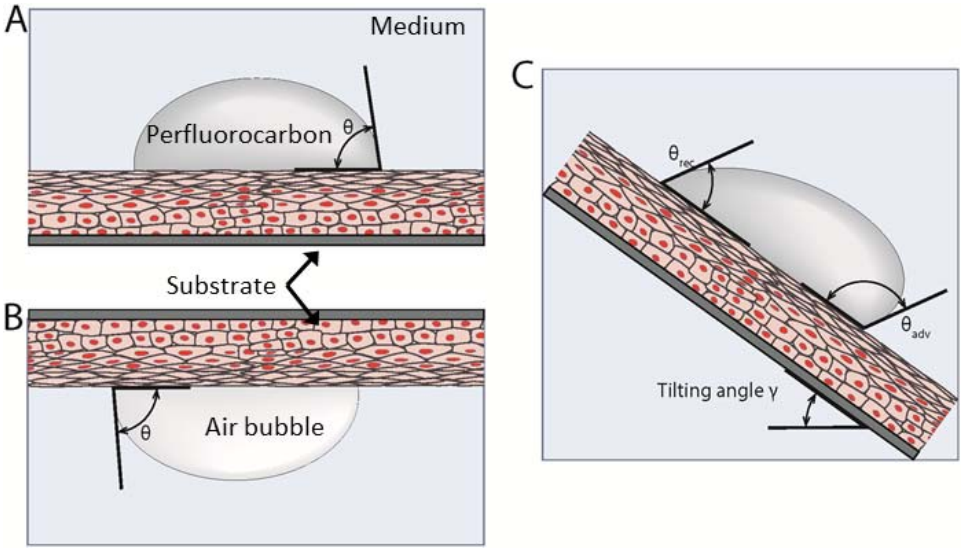


**Figure 1.** (**A**) Use of two-liquid method to measure contact angle. In this system, the bulk fluid is PBS and the droplet is a perfluorocarbon. (**B**) Captive bubble method used to measure contact angle. (**C**) Tilting of the apparatus to measure the advancing and receding contact angles.

misleading because the thin film of liquid covering the surface on hydrated cells impedes the measurement of an angle. Furthermore, if the cell surface is allowed to dry, the contact angle changes values, depending on the moisture level, as observed by Tiffany,[7] suggesting the loss of the native state of the cell's surface. To overcome some of the challenges intrinsic to using water as the probe, other liquids can be used to characterize surfaces, such as polar liquids (e.g., glycerol or formamide) or nonpolar lipids (e.g., diiodomethane or benzene). However, polar liquids can disturb the cells due to the difference in osmolarity between the liquid and the cytosol, whereas many nonpolar liquids interact with the phospholipids of the cellular membrane, disrupting it.[13] Therefore, the choice of fluid(s) used to measure contact angles of cell surfaces bathed in a fluid environment is critical in determining the interfacial properties. In this work, we used the two-liquid system, where cells are immersed in an isotonic physiologic buffer, and the contact angle is recorded using a nonreactive nonpolar liquid (perfluorocarbon) deposited on the cell surface (Fig. 1A). We also performed the captive bubble method, where the surface of interest is inverted and an air bubble is trapped in contact with the surface (Fig. 1B). Both of these methods permit the measurement of the contact angle and the contact angle hysteresis, which is a measurement that correlates to the uniformity of the surface. For smooth and uniform surfaces, droplets have unique contact angles. However, on heterogeneous surfaces, such as biological surfaces, droplets become pinned by defects and possess an advancing and a receding angle of contact, which may be recorded by tilting the apparatus (Fig. 1C). The intrinsic biochemical make up and surface topography of the ocular surface contribute to this heterogeneity, and the extent to which this promotes the retention of the tear film at the ocular surface is understudied. These measurements allow evaluation of the surface properties at different maturation levels of the glycocalyx during the stratification process of immortalized human corneal epithelial cells.

## Methods

### Cell Culture

Human telomerase reverse transcriptase-immortalized corneal epithelial (hTCEpi) cells were graciously donated by James Jester, PhD (University of California Irvine).[11] Cells were used between passages 50 and 60. hTCEpi cells were cultured in growth medium (GM) composed of Epilife (LifeTechnologies, Carlsbad, CA, USA) supplemented with Epilife defined growth supplement (a proprietary combination of bovine serum albumin, bovine transferrin, hydrocortisone, recombinant human-like growth factor type-1, prostaglandin, and recombinant human epidermal growth factor [Life Technologies]). Cells were incubated on the surface of glass slides treated with a proprietary mixture of fibronectin-collagen coating (Athena Enzyme Systems, Baltimore, MD, USA) as described previously[14,15] at 37°C and 5% $CO_2$, until they reached 100% confluence, and the GM was replaced by stratification medium (SM) containing Dulbecco modified Eagle/F12 medium (Invitrogen, Carlsbad, CA, USA), 10% fetal bovine serum, 10 ng/mL EGF, 100 units of penicillin, and 100 μg/mL streptomycin to induce differentiation and stratification.[10]

### Quantitative Polymerase Chain Reaction (Q-PCR)

Total RNA was extracted from three replicates for hTCEpi cells cultured to 100% confluence in GM and for hTCEPi cells cultured in SM at days 1 through 7, following the Qiagen RNeasy kit protocol (Qiagen, Germantown, MD, USA). Briefly, cells were lysed in 350 μL of RLT buffer (Qiagen) containing 10 μL/mL of 2-mercaptoethanol (Sigma-Aldrich Corp., St. Louis, MO, USA). An equal amount of 70% ethanol was added to each sample and mixed prior to loading onto H-Bind columns (Qiagen). Columns were washed with buffers RW1 and RPE (Qiagen) and eluted with 30 μL of nuclease-free water. Sample concentrations were measured at an optical density (OD) of 260 nm for total RNA, using a NanoDrop 2000 spectrophotometer (Thermo Scientific, Wilmington, DE, USA). The concentration of RNA was calculated using the equation $[C = (A * \varepsilon)/b]$, where $C$ is the nucleic acid concentration (ng/μL), $A$ is the absorbance at 260 nm, $\varepsilon$ is the extinction coefficient (40 ng/cm/μL for RNA), and $b$ is the path length in centimeters. Samples were further diluted with nuclease-free water to a concentration of 75 ng/mL and stored at −20°C.

Primers were purchased from the predeveloped and commercially available TaqMan assay reagents (LifeTechnologies), and the assay kits used were: MUC1 assay ID Hs00159357-m1 (GenBank reference sequence AF125525.1;

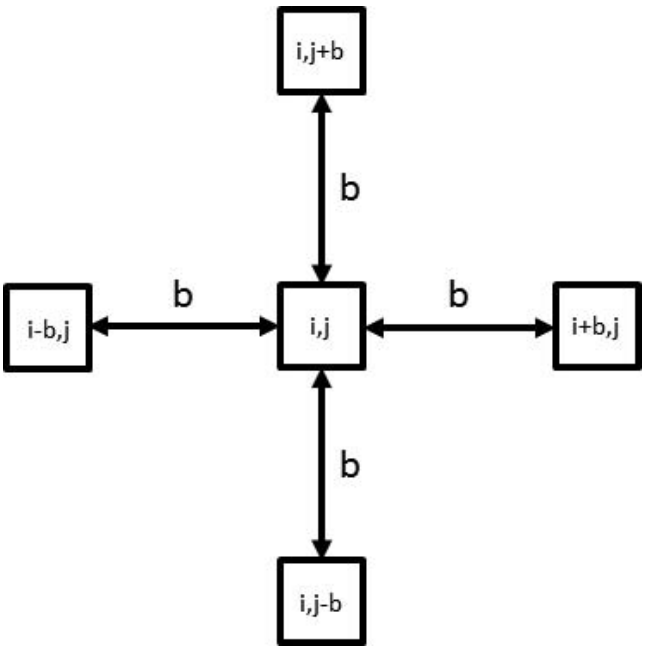


FIGURE 2. Pentuplet quadrat variance (5QV) method. The variance between the intensity of the central pixel (*i*, *j*) and the pixels at distance *b* on the four cardinal points was calculated.

exon boundary, 7–8; assay location, 684; amplicon length = 84 bp)[16]; MUC4 assay ID Hs00366414-m1 (GenBank reference sequence, AJ010901.1; exon boundary, 16–17; assay location, 2215; amplicon length = 55 bp); MUC16 assay ID Hs01065189-m1 (GenBank reference sequence AK024365.1; exon boundary, 33–34; assay location, 3251; amplicon length = 63 bp); and 18S assay ID Hs99999901-s1 (GenBank reference sequence, X03205.1; exon boundary, 1–1; assay location, 604; amplicon length = 187 bp). Quantitative PCR was performed using SensiFAST probe Hi-ROX one-step kit (Bioline, Taunton, MA, USA), applying 75 ng of total RNA per sample, using a StepOne RT-PCR system (Applied Biosystems, Carlsbad, CA, USA). Reaction conditions were 50°C for 20 minutes, 95°C for 10 minutes; and 40 cycles of 95°C for 15 seconds and 60°C for 1 minute. Quantification of relative gene expression was performed using the $\Delta\Delta Ct$ method,[17] using StepOne real-time PCR software (Applied Biosystems). Blank controls were run to ensure specificity of the amplifications.

## Western Blotting

Cell cultures were washed once in phosphate-buffered saline (PBS) and lysed and scraped into 2% sodium dodecyl sulphate (Fisher, Tokyo, Japan) in PBS, supplemented with Halt protease and phosphatase inhibitor cocktail (Thermo Scientific). Cells were homogenized and centrifuged at 1000*g* for 1 minute to remove cell debris. Protein was quantified by using a modified Lowry assay (DC assay; Bio-Rad Laboratories, Hercules, CA, USA), using bovine serum albumin as the standard. Protein homogenate was denatured in NuPAGE lithium dodecyl sulfate (LDS) sample buffer (Life Technologies), and 50 µg protein was loaded onto 0.7% agarose gels (SeaKem LE agarose; Lonza, Rockland, ME, USA) and transferred onto a polyvinylidene fluoride (Immobilon-P; Millipore, Billerica, MA, USA). The membrane was blocked for 2 hours at 25°C in milk diluent/blocking (KPL, Gaithersburg, MD, USA). The antibodies used for immunoblotting were anti-human MUC1/episialin clone 214D4 (Millipore), MUC4 clone 8G7 (Abcam, Cambridge, MA, USA), and MUC16 clone OC125 (Abcam) for 1 hour at 37°C. This was followed by incubation with horseradish peroxidase–labeled goat anti-mouse antibody (KPL) for 1 hour at 25°C, and the bands were detected by chemiluminescence (Western-bright Quantum Western blotting detection for horseradish-peroxidase conjugates; Advansta, Menlo Park, CA, USA) and imaged using ChemiDoc-It imaging system (UVP, Upland, CA, USA).

## Contact Angle/Surface Energy and Hysteresis

Contact angles were determined using a Ramé-Hart model 290 contact angle goniometer (Rame-Hart Instruments, Succasunna, NJ, USA) equipped with an environmental fixture and an automated tilting base. Surfaces were placed in the environmental fixture filled with Dulbecco PBS (DPBS). For captive bubble measurements, the cellular surfaces were placed facing down and for sessile droplet measurements with perfluorocarbons (perfluorodecalin, perfluorooctane, and tetradecafluorohexane [Sigma-Aldrich Corp.]), the cellular surfaces were placed facing up. The choice of perfluorocarbons was based on their insolubility in aqueous solutions, their nontoxicity, their inertness, and their precedent usage for biomedical applications.[18–20] The air bubbles or perfluorocarbon droplets (10 µL) were placed in contact with the cellular surface. The stage was tilted at a rate of 0.5°/s, and the advancing and receding angle values were measured every second until the bubble/droplet rolled off the surface. The hysteresis of the contact angle was determined by recording the advancing (*adv*) and receding (*rec*) angles at the moment just before the droplet rolled off and calculating the difference of the cosine of both angles [cos $\theta_{adv}$ − cos $\theta_{rec}$].[21] According to Furmidge,[22] the value of [cos $\theta_{adv}$ − cos $\theta_{rec}$] when the droplet starts to slide is a constant, independent of the size of the droplet and the angle of tilt.

## Atomic Force Microscopy (AFM)

Cells were fixed in 5% glutaraldehyde and 4% paraformaldehyde in DPBS for 30 minutes, washed in DPBS, and imaged by atomic force microscopy (AFM), using the MFP-3D BIO AFM (Asylum Research, Santa Barbara, CA, USA) coupled with an Axio Observer inverted microscope (Carl Zeiss, Thornwood, NY, USA). Imaging was performed in fluid contact mode, using silicon nitride cantilevers (catalog no. PNP-TR-50, nominal spring constant [k] of 0.22 N/m and half angle opening of 35°; NanoAndMore, Lady's Island, SC, USA) at an applied force of 500 pN and 0.3 Hz. Root-mean-square (RMS) values were extracted from the images by using built-in functions of Asylum Research AFM version 12 software (Oxford Instruments, Scotts Valley, CA, USA).

## Labeling of O-glycans on the Cell Surface

To label the O-glycans on the surface of the cell cultures, the cell cultures were incubated with 10 µg/cm$^2$ of biotinylated jacalin (Vector Labs, Burlingame, CA, USA), a plant-based lectin, for 30 minutes, followed by rinsing with DPBS. The cells were then cultured in 0.625 µM of SYTO11 nuclear dye (Molecular Probes, Eugene, OR, USA) supplemented with 5 µL/mL streptavidin-conjugated quantum dots (Qdot 585; Molecular Probes) for 30 minutes. Cultures were then rinsed twice with DPBS, and examined using using epifluorescence microscopy (Zeiss). Controls using competitive inhibition with 1 mM β-lactose (Sigma-Aldrich Corp.) and noncompetitive controls with 1 mM sucrose (Sigma-Aldrich Corp.) were used to ensure specificity of binding of jacalin to β-galactosides. For binding, 10 µg/cm$^2$ of biotinylated bovine serum albumin (BSA; Sigma-Aldrich Corp.) was used as nonspecific binding controls.

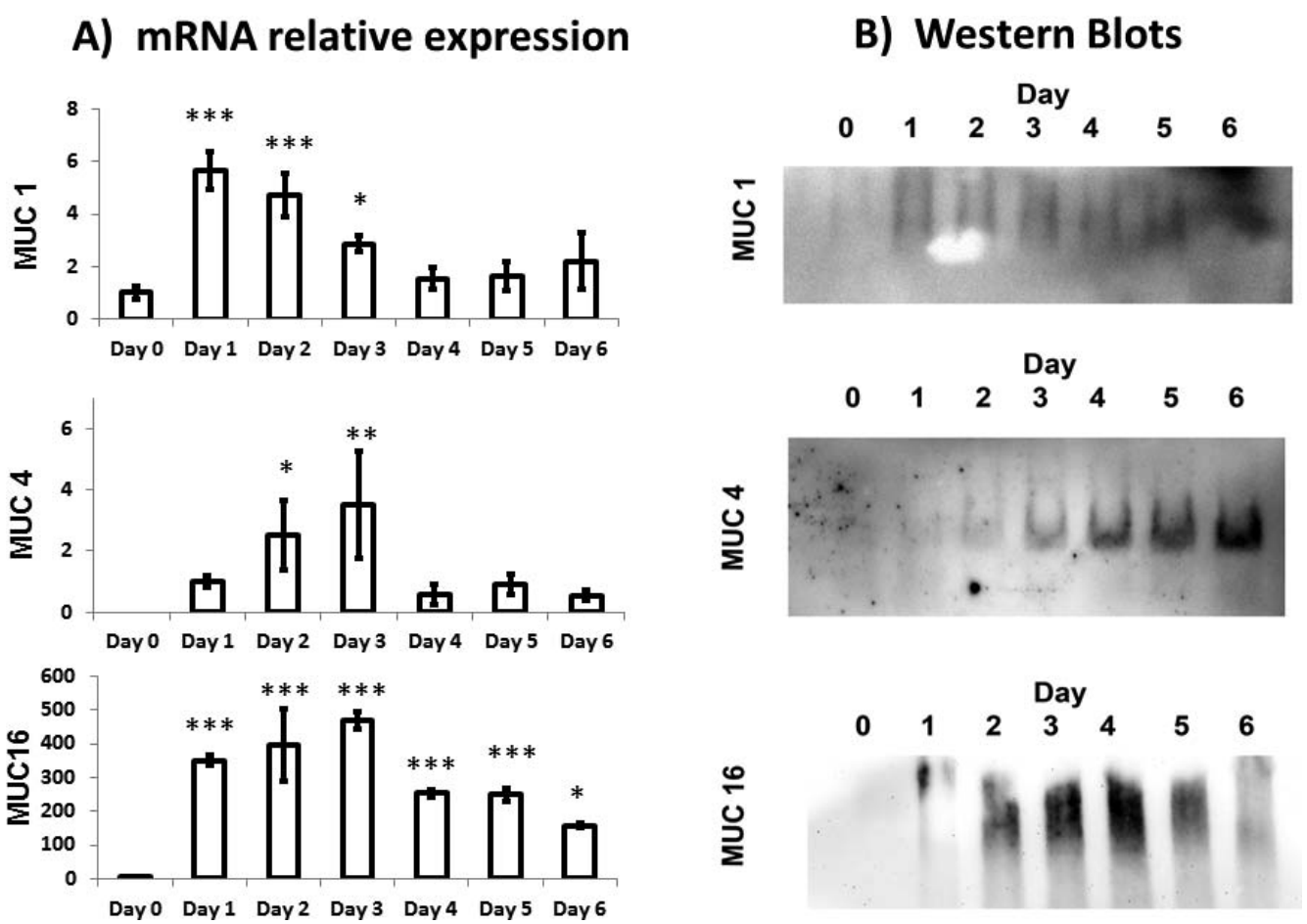


FIGURE 3. (**A**) Relative mucin mRNA expression for the hTCEpi cell cultures at day 0 (unstratified cells) and at days 1 to 6 during the stratification process. For unstratified cells, the expression of MUC1 was low, and the expression levels of MUC4 and MUC16 were negligible. Expression of mucin mRNA reached a peak between day 1 and day 3 ($n = 3$). *Error bars* = standard deviations. Significance with respect to undifferentiated cells: $^{***}P \leq 0.001$; $^{**}P \leq 0.01$; $^{*}P \leq 0.05$. (**B**) Western blot analysis showed expression of the mucin protein for hTCEpi cell cultures at day 0 (unstratified cells) and at days 1 to 6 during the stratification process. For unstratified cells, expression of all mucins is negligible. Expression levels of the proteins MUC1 and MUC16 reproduced the observed mRNA expression profile, whereas expression of the MUC4 protein suggested a monotonic increase during the stratification process.

### Statistical Analysis

Experiments were analyzed using 1-way analysis of variance (ANOVA). When variability was determined to be significant ($P < 0.05$), the Tukey multiple comparison test was performed to determine significance between groups.

The heterogeneity and scale of the pattern of distribution of glycosylated molecules was measured using the pentuplet quadrat variance method (5QV).[23] This method computes the variance between a pixel and the pixels that are at distance $b$ from the initial one on the 4 cardinal points (Fig. 2). The variance $V_5(b)$ for each $b$ value is

$$V_5(b) = \frac{\sum_{i=b+1}^{n_x-b}\sum_{j=b+1}^{n_y-b}(d_{i-b,j} + d_{i+b,j} + d_{i,j-b} + d_{i,j+b} - 4d_{i,j})^2}{20(n_x - 2b)(n_y - 2b)},$$

where $n_x$ is the number of pixels in the $x$-axis and $n_y$ is the number of pixels in the $y$-axis. The variance is charted relative to several $b$ distances. The higher the variance, the more heterogeneous the surface is, and peaks on the variance are correlated to the scale of the patterning. The pixel size of the images analyzed with the 5QV method was of 0.32 μm/pixel.

## RESULTS

### Mucin Expression

Stratification of hTCEpi cells was induced when cultured in SM (see Supplementary Fig. S1 for stratified cultures). Q-PCR was used to evaluate the mRNA expression of the most relevant mucins of the ocular surface (MUC1, MUC4, and MUC16) during the differentiation and stratification process. Undifferentiated hTCEpi cells showed little MUC1 mRNA expression and negligible MUC4 and MUC16 expression (Fig. 3A, day 0). When the GM was replaced by SM, hTCEpi cells markedly increased expression of all three cell-associated mucin genes (Fig. 3A, days 1–6) with maximum expression seen between days 1 and 3.

Mucin protein expression levels were validated by Western blot analysis. Due to the large size of mucin proteins, the smaller proteins such as those used as endogenous controls were lost during electrophoresis; thus our evaluation of protein expression was qualitative. MUC1 and MUC16 expression profiles reflected the findings for mRNA expression, with maximum expression between days 1 and 3 and then a decrease between days 4 and 6 (Fig. 3B). Protein expression of MUC4 was observed to continuously increase up

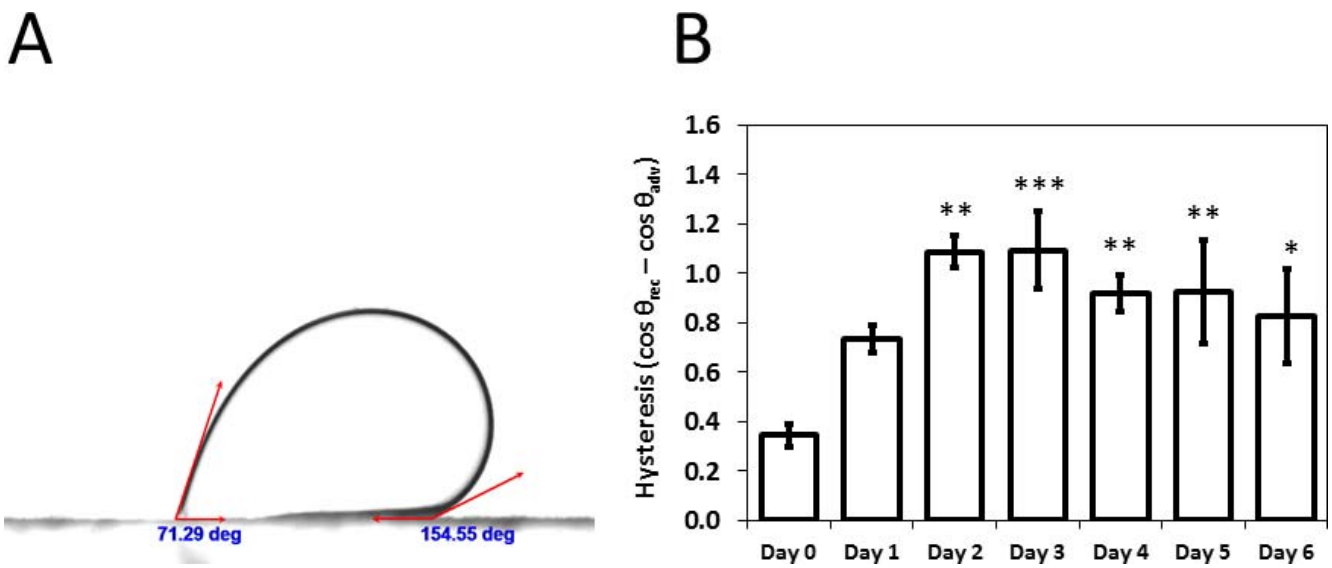


FIGURE 4. (**A**) Contact angle hysteresis. The surface is tilted, and the advancing (highest) contact angle and receding (lowest) contact angle are recorded at the point where the droplet starts to slide. (**B**) Contact angle hysteresis of perfluorodecalin droplets for the cell cultures at day 0 (unstratified) and at days 1 to 6 during the stratification process. Hysteresis reached a peak between day 2 and 3 and then decreased, similar to the expression profile of mucins ($n = 3$). *Error bars* = standard deviations. Significance with respect to undifferentiated cells: $^{***}P \leq 0.001$; $^{**}P \leq 0.01$; $^{*}P \leq 0.05$.

to day 6 (Figure 3B) in contrast with its mRNA expression profile (Fig. 3A).

## Contact Angle and Contact Angle Hysteresis

To test whether the changes in surface mucin expression influenced the wettability of the corneal epithelium, we devised a two-liquid method to measure the contact angle. The cell cultures were immersed in PBS, with the cell surface of the substrates facing down in the case of captive air bubbles and facing up for sessile perfluorocarbon drops. On first inspection, the measured contact angles (initial static contact angle) were similar between all samples, from day 0 to day 6 (145°–150°). However, when the surfaces were tilted, we observed a very significant increase in the contact angle hysteresis for the cells cultured in SM, compared to that for the unstratified cells cultured in GM (Fig. 4A; see also Supplementary Video S1). To illustrate this behavior, in Figure 4B, we show the contact angle hysteresis profile of perfluorodecalin droplets, where the hysteresis observed to increase to a maximum for the SM cells between days 2 and 3, before progressively decreasing. This profile very closely mimicked the mucin expression profile. For perfluorooctane droplets, tetradecafluorohexane droplets, and air bubbles, the hysteresis profile was identical to the perfluorodecalin droplets (Supplementary Material).

## Topography

To elucidate the possible cause for the large change in hysteresis of the contact angle, we evaluated the surface topography of hTCEpi cells at different stratification levels, imaging the cells by using AFM. hTCEpi cells cultured on GM showed a cobblestone morphology with tall and discrete polygonal cells. Once exposed to SM, the topmost layer of cells appeared flatter with well-marked cell junctions. Except for some very small surface protrusions, no other topographic feature was apparent in those images (Fig. 5). The mean ± standard deviation RMS value for control epithelial cells (day 0) in GM was approximately 1060 ± 120 nm, whereas the values for cells in SM on day 1 was 470 ± 80 nm; 450 ± 120 nm on Day 2; 500 ± 80 nm on day 3; 530 ± 90 nm on day 4; 580 ± 110 nm on Day 5′ and 460 ± 30 nm on day 6 (Supplementary Fig. S3). These figures showed a significant flattening of cells once the medium was changed to SM. No significant differences in roughness were observed between the culture day of cells cultured in SM.

## Surface Glycosylation Heterogeneity

To determine the expression and spatial distribution of glycoproteins on the corneal epithelium surface, hTCEpi cells at different degrees of differentiation were incubated with jacalin-Qdots (for O-glycans) or BSA-Qdots (as a nonspecific binding control) and imaged for epifluorescence. Unstratified cells demonstrated very little yet uniformly distributed jacalin binding. However, cells cultured in SM showed a dramatic change in both the extent of jacalin binding and the heterogeneity of the surfaces (Fig. 6). The lactose-supplemented controls inhibited binding of the Qdots to the surface glycosides, whereas the sucrose-supplemented controls did not inhibited the binding, demonstrating specificity of jacalin to β-galactosides. The controls using BSA showed no nonspecific binding (data not shown).

Quantification of the surface heterogeneity with the quadrat variance method shows that the surface distribution of mucins of unstratified cells is homogeneous (flat curve with low variance), whereas the spatial heterogeneity dramatically increases with stratification. The maxima of the variance indicate the scale of the glycosylated patches (20–80 μm, which roughly corresponds to the diameter of the cells) (Fig. 7). This suggests that among the population of surface cells, certain cells dramatically upregulate mucin expression, whereas others do not.

# DISCUSSION

Although one of the roles attributed to membrane-associated mucins of the corneal epithelium (mainly MUC1, MUC4, and MUC16)[9] has been to facilitate the wettability of the corneal

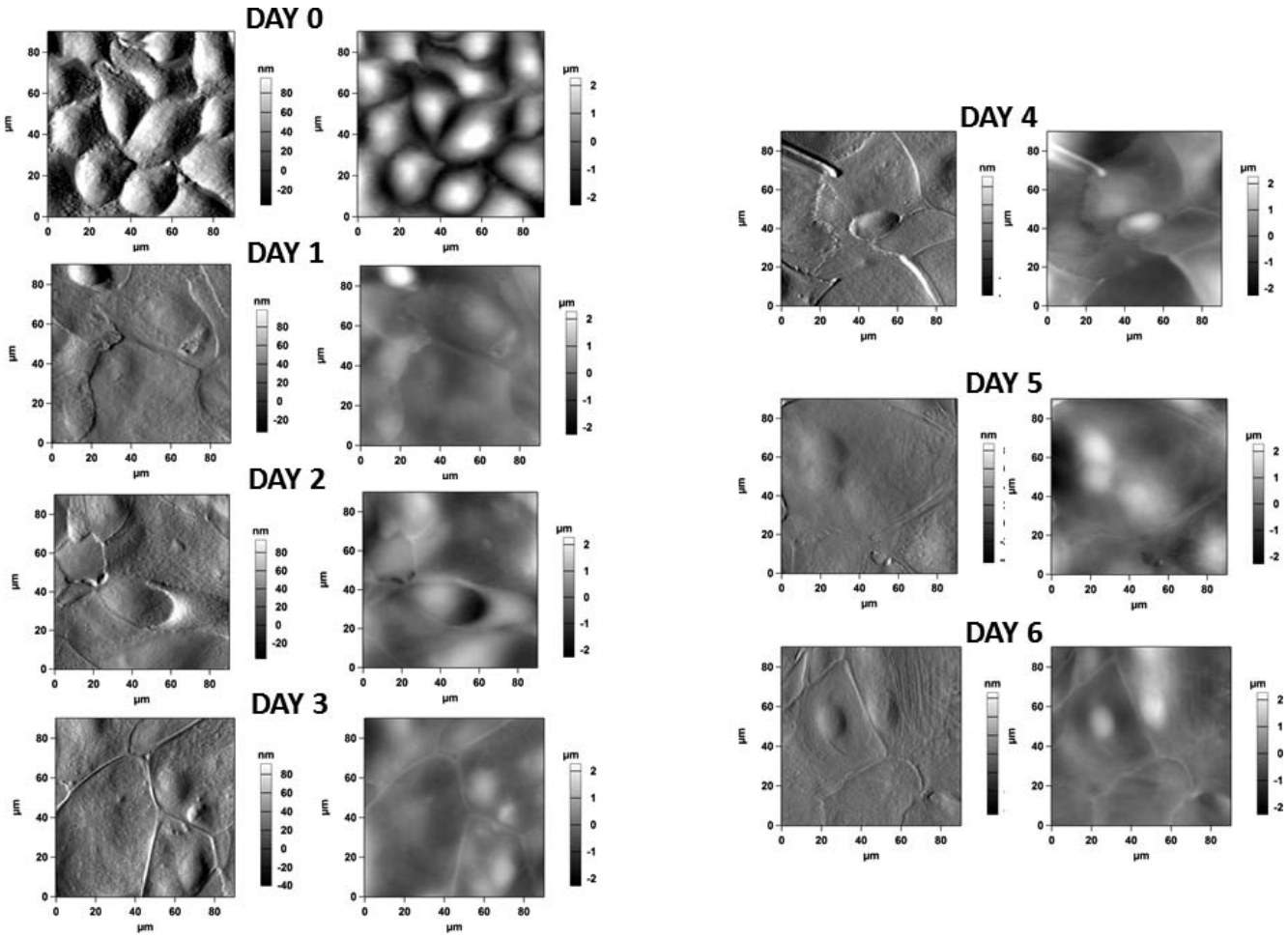


FIGURE 5. Atomic force microscopy images of the cell cultures at day 0 (unstratified) and at days 1 to 6 during the stratification process. (*Left*) Figures represent phase images; (*right*) figures represent height images. Unstratified cells show cobblestone morphology, and are tall with no discernable cell junctions, resembling basal corneal epithelial cells. Once exposed to SM, cells flatten and develop marked cell junctions. No other noticeable topographic features were observed.

epithelium,[24–26] most studies involving measurements of hydrophilicity of the ocular surface do not directly test this hypothesis.[5–7] The principal aim of this work was to correlate the wetting characteristics of the corneal epithelium in a hTERT cell line (HTCEpi cells) with the surface expression and spatial distribution of the cell associated mucins.

Although another immortalized hTERT corneal epithelium (HCLE) and a conjunctival epithelium (HCjE) cell line have been tested for mucin expression[27] and exhibited the mucin repertoire characteristic of the native epithelium (albeit at lower mRNA levels), to our knowledge, the hTCEpi immortalized corneal epithelial cell line has not been previously characterized with respect to mucin expression.[11] We observed a time-dependent increase in mucin expression during the first 3 days and then a decrease thereupon (confirmed through mRNA and protein). Hori el al.[28] analyzed the expression profile of HCjE cells during the stratification process up to 3 days and observed an increase in mucin expression, albeit with an independent pattern of regulation, similar to the first 3 days of our experiments. Furthermore, similar to our results, Hori et al.[28] also observed low but detectable levels of MUC1 and MUC16 mRNA in unstratified cultures and no detectable expression of MUC4. Further studies will indeed be required to validate our findings in vivo. In our experiments, the mRNA expression profiles for MUC1 and MUC16 corresponded to their protein expression profile. In contrast, for MUC4, mRNA expression peaked at day 3, but there was a monotonic increase in protein expression up to day 6, which may reflect a very low turnover of MUC4 in the cell cultures.

Once the expression profile of mucins was established, the surface properties of the cell cultures were characterized by the measurement of contact angles. The contact angle is a thermodynamic property.[29] However, our observation of a very high contact angle hysteresis indicated a nonequilibrium state of droplets on the cellular surface and therefore prevented the measurement of a meaningful single surface energy.[29,30] Nonetheless, this large contact angle hysteresis on cells subjected to the stratification process indicates the presence of "defects" on the surface, to which the droplets are pinned, impeding the advancement and retraction of the droplet and generating a difference in the advancing and receding contact angles.[30] The development of this contact angle hysteresis suggests the development of spatial surface heterogeneities with the most likely possibilities being the development of spatially discrete topographic features[31] or surface chemistry functionality[32] on the cell cultures. Furthermore, the hysteresis profile matches both the mucin expression and the surface heterogeneity of the cell cultures, pointing to the impact of mucins on this surface phenomenon.

To determine whether rugosity (amplitude of surface topographic features) contributed to the hysteresis of the

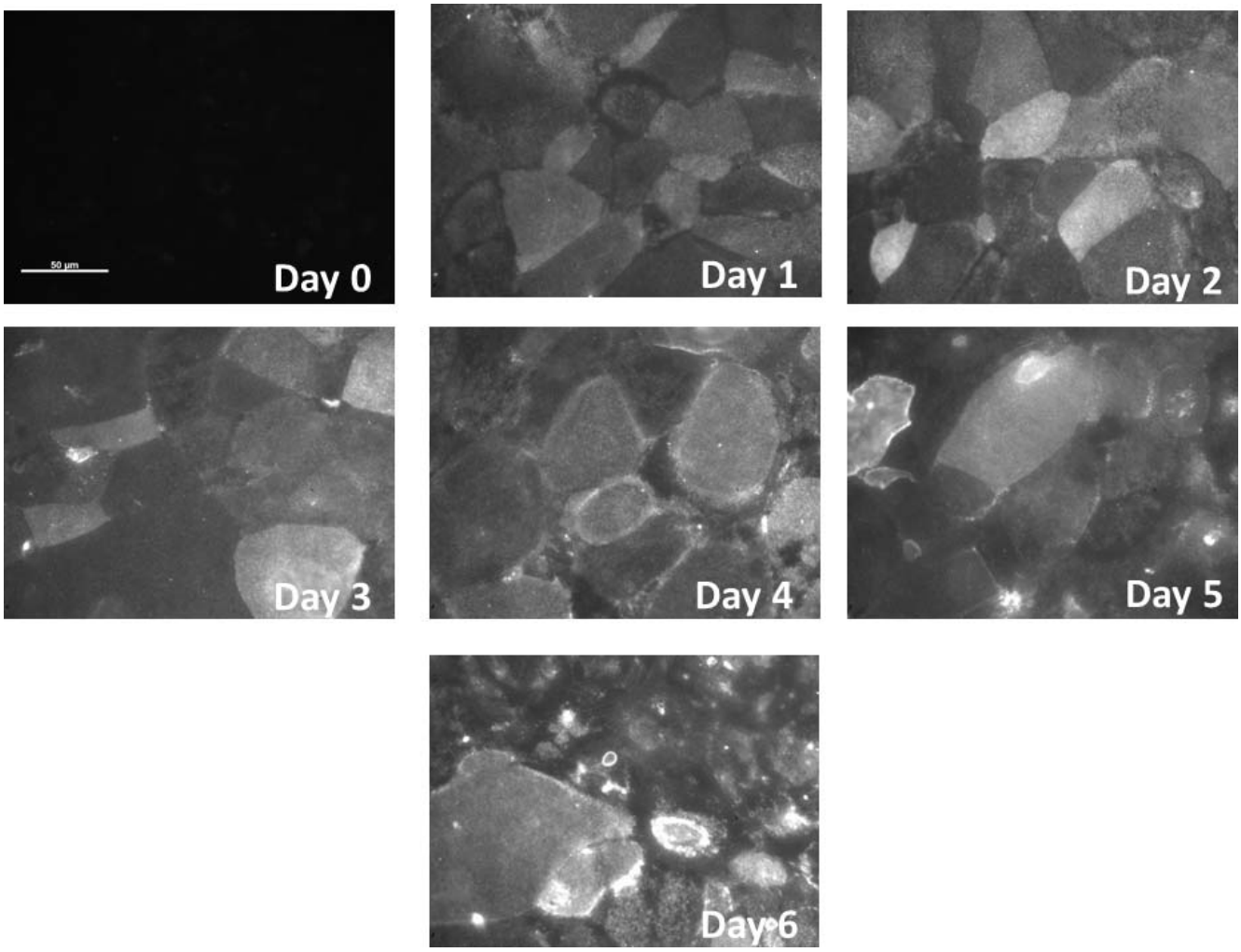


FIGURE 6. Surface O-glycosylation visualized with fluorescent jacalin for the hTCEpi cell cultures at day 0 (unstratified cells) and at days 1 to 6 during the stratification process. Jacalin binding for unstratified cells is low and appears to be uniformly distributed. Staining increases when the stratification process starts, showing high heterogeneity of the surface O-glycosylation. *Scale bar*: 50 µm.

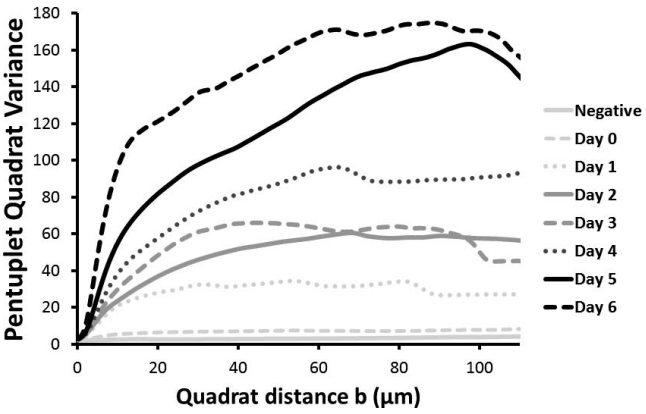


FIGURE 7. Pentuplet quadrat variance (5QV) of the fluorescent jacalin cell cultures at day 0 (unstratified) and at days 1 to 6 during the stratification process. Variance represents the surface O-glycosylation heterogeneity. Unstratified cells showed very little heterogeneity, and this increased with the differentiation process. The maxima of the graphs correlated with the size of the heterogeneities.

contact angle, we imaged the culture surface using AFM (Supplementary Fig. S3). Surface roughness does not change substantially once the cells are plated in stratification medium. The RMS value of the surface is significantly reduced between day 0 (in GM) and day 1 (in SM) and remains fairly stable up to day 6 (in SM). We noted significant flattening of superficial epithelial cells with stratification. The unstratified cells showed a cobblestone morphology, with tall and distinct cells resembling the morphology of basal corneal epithelial cells,[33] while the stratified cultures showed a very flat surface consistent with the flattened, squamous apical epithelial surface cells.[33] It would be anticipated that the development of surface topography would contribute to the increase of contact angle hysteresis observed in our experiments; however, similar RMS values of cells in SM strongly suggest other factors as the source of the observed increase in hysteresis upon differentiation.

To elucidate the surface elements affecting the high contact angle hysteresis in stratified cells, we also tested the distribution of glycosylated proteins on the surface of the cell cultures by imaging with fluorescently tagged jacalin. Jacalin is a plant-based lectin found in jackfruits that binds to Gal/GalNAc and is considered a prime candidate to generically select O-glycans.[34] Jacalin has been reported to bind intracel-

lularly to the perinuclear region in HCLE cells.[35] To minimize the internalization of the reporter dyes, we designed an assay using streptavidin-coated Qdots that were not membrane permeable[36] and ensured the binding to the O-glycans decorating the cell surface. We observed major differences in the distribution of O-glycans on the cell surface between undifferentiated and stratified cells. Notably, a "mosaic" pattern was observed in stratified cell cultures. Such a pattern has been observed previously and correlated to normal eyes in vivo, while pathologic patterns (such as a "starry sky pattern") correspond to dry eye patients,[26,37] suggesting that the heterogeneity of the surface chemistry of the ocular surface may play an important role in dry eye syndrome. Considering that high contact angle hysteresis is linked to the pinning of the contact line,[32] this phenomenon may also influence the "dewetting" of the tear film by stabilizing the contact line between the ocular surface and the aqueous tear film, impeding the initiation and expansion of dry patches. Future experiments involving measurements obtained in vivo need to be performed to determine the influence of soluble biomolecules and lipids on contact angle hysteresis evidenced by the ocular surface.

In summary, we have developed a method to characterize biophysical surface properties on cell cultures by measuring the contact angle and contact angle hysteresis with two liquids, ensuring the normal level of hydration of the cell surface and avoiding disruption of the chemical components of the cellular membrane. The high value of contact angle hysteresis in our cell cultures precluded us from obtaining meaningful values for surface energy. However, the same large contact angle hysteresis informs us about the development of surface functional heterogeneity of mucin expression and spatial distribution with differentiation of corneal epithelial cells. To our knowledge, this is the first report of contact angle hysteresis on the corneal epithelium. The magnitude of the contact angle hysteresis is related to a "retentive force" that stabilizes and pins droplets in an inclined plane.[38] This retentive force may play an important role in the stability/instability of liquid films on the ocular surface, and it could have a major implication on the development of dry eye syndromes. Therefore, we hypothesize that differences in contact angle hysteresis may potentially be used to diagnose the health of the ocular surface and that, by engineering the surface properties of the corneal and conjunctival epithelia, we could increase the stability and retention of the tear film on the ocular surface.

## *Acknowledgments*

The authors thank Brad Rose, Josh Morgan, PhD, Paul Russell, PhD, and Sophia Fang, MD, MS, for their excellent technical support and meaningful discussions.

Supported by National Eye Institute, National Institutes of Health Grants RO1EY016134 (CJM), RO1EY019970 (CJM), and P30EY012576 (JSW). The study was partially supported by Grant VAF2014-02 to BCL from ACVO Vision for Animal Foundation.

Disclosure: **B. Yáñez-Soto**, None; **B.C. Leonard**, None; **V.K. Raghunathan**, None; **N.L. Abbott**, None; **C.J. Murphy**, None

## *References*

1. Lemp MA, Foulks GN. The definition and classification of dry eye disease. *Ocul Surf*. 2007;5:75–92.
2. Schaumberg DA, Sullivan DA, Buring JE, Dana MR. Prevalence of dry eye syndrome among US women. *Am J Ophthalmol*. 2003;136:318–326.
3. Schaumberg DA, Dana R, Buring JE, Sullivan DA. Prevalence of dry eye disease among US men: estimates from the Physicians' Health Studies. *Arch Ophthalmol*. 2009;127:763–768.
4. Yañez-Soto B, Mannis MJ, Schwab IR, et al. Interfacial phenomena and the ocular surface. *Ocul Surf*. 2014;12:178–201.
5. Holly FJ, Lemp MA. Wettability and wetting of corneal epithelium. *Exp Eye Res*. 1971;11:239–250.
6. Sharma A. Surface properties of normal and damaged corneal epithelia. *J Dispers Sci Technol*. 1992;13:459–478.
7. Tiffany JM. Measurement of wettability of the corneal epithelium. *Acta Ophthalmol*. 1990;68:175–181.
8. Johnson ME, Murphy PJ. Changes in the tear film and ocular surface from dry eye syndrome. *Prog Retin Eye Res*. 2004;23:449–474.
9. Gipson IK, Argüeso P. Role of mucins in the function of the corneal and conjunctival epithelia. *Int Rev Cytol*. 2003;231:1–49.
10. Argüeso P, Gipson IK. Assessing mucin expression and function in human ocular surface epithelia in vivo and in vitro. In: McGuckin M, Thornton D, eds. *Mucins. Methods and Protocols*. Philadelphia, PA: Springer; 2012:313–325.
11. Robertson DM, Li L, Fisher S, et al. Characterization of growth and differentiation in a telomerase-immortalized human corneal epithelial cell line. *Invest Ophthalmol Vis Sci*. 2005;46:470–478.
12. Lemp MA, Holly F, Iwata S, Dohlman C. The precorneal tear film. *Arch Ophthalmol*. 1970;83:89–94.
13. Cope C, Dilly P, Kaura R, Tiffany J. Wettability of the corneal surface: a reappraisal. *Curr Eye Res*. 1986;5:777–785.
14. Raghunathan V, McKee C, Cheung W, et al. Influence of extracellular matrix proteins and substratum topography on corneal epithelial cell alignment and migration. *Tissue Eng Part A*. 2013;19:1713–1722.
15. McKee CT, Raghunathan VK, Nealey PF, Russell P, Murphy CJ. Topographic modulation of the orientation and shape of cell nuclei and their influence on the measured elastic modulus of epithelial cells. *Biophys J*. 2011;101:2139–2146.
16. Robinson MB, Deshpande DA, Chou J, et al. IL6 trans-signaling increases expression of airways disease genes in airway smooth muscle. *Am J Physiol Lung Cell Mol Physiol*. 2015;309:L129–L138.
17. Livak KJ, Schmittgen TD. Analysis of relative gene expression data using real-time quantitative PCR and the $2^{-\Delta\Delta CT}$ method. *Methods*. 2001;25:402–408.
18. Spieth PM, Knels L, Kasper M, et al. Effects of vaporized perfluorohexane and partial liquid ventilation on regional distribution of alveolar damage in experimental lung injury. *Intensive Care Med*. 2007;33:308–314.
19. Claes C, Worst J, Zivojnovic R. Retinal detachment surgery following implantation of a keratoprosthesis. A case report. *Bull Soc Belge Ophtalmol*. 1991;243:167–169.
20. Ferenz KB, Waack IN, Laudien J, et al. Safety of poly(ethylene glycol)-coated perfluorodecalin-filled poly (lactide-co-glycolide) microcapsules following intravenous administration of high amounts in rats. *Results Pharma Sci*. 2014;4:8–18.
21. Extrand C, Kumagai Y. An experimental study of contact angle hysteresis. *J Colloid Interface*. 1997;191:378–383.
22. Furmidge C. Studies at phase interfaces. I. The sliding of liquid drops on solid surfaces and a theory for spray retention. *J Colloid Sci*. 1962;17:309–324.
23. Fortin M-J, Dale MRT. *Spatial Analysis: A Guide for Ecologists*. Cambridge, UK: Cambridge University Press; 2005.

24. Watanabe H. Significance of mucin on the ocular surface. *Cornea*. 2002;21:S17–S22.
25. Guzman-Aranguez A, Argüeso P. Structure and biological roles of mucin-type O-glycans at the ocular surface. *Ocul Surf*. 2010;8:8–17.
26. Argüeso P, Gipson IK. Epithelial mucins of the ocular surface: structure, biosynthesis, and function. *Exp Eye Res*. 2001;73: 281–289.
27. Gipson IK, Spurr-Michaud S, Argüeso P, Tisdale A, Ng TF, Russo CL. Mucin gene expression in immortalized human corneal-limbal and conjunctival epithelial cell lines. *Invest Ophthalmol Vis Sci*. 2003;44:2496–2506.
28. Hori Y, Spurr-Michaud S, Russo CL, Argüeso P, Gipson IK. Differential regulation of membrane-associated mucins in the human ocular surface epithelium. *Invest Ophthalmol Vis Sci*. 2004;45:114–122.
29. Berg JC. *An Introduction to Interfaces and Colloids: The Bridge to Nanoscience*. Singapore: World Scientific; 2010.
30. Gao L, McCarthy TJ. Contact angle hysteresis explained. *Langmuir*. 2006;22:6234–6237.
31. Ramos S, Charlaix E, Benyagoub A. Contact angle hysteresis on nano-structured surfaces. *Surf Sci*. 2003;540:355–362.
32. Extrand C. Contact angles and hysteresis on surfaces with chemically heterogeneous islands. *Langmuir*. 2003;19:3793–3796.
33. Gospodarowicz D, Greenburg G, Birdwell C. Determination of cellular shape by the extracellular matrix and its correlation with the control of cellular growth. *Cancer Res*. 1978;38:4155–4171.
34. Tachibana K, Nakamura S, Wang H, et al. Elucidation of binding specificity of Jacalin toward O-glycosylated peptides: quantitative analysis by frontal affinity chromatography. *Glycobiology*. 2006;16:46–53.
35. Argüeso P, Tisdale A, Spurr-Michaud S, Sumiyoshi M, Gipson IK. Mucin characteristics of human corneal-limbal epithelial cells that exclude the Rose Bengal anionic dye. *Invest Ophthalmol Vis Sci*. 2006;47:113.
36. Howarth M, Takao K, Hayashi Y, Ting AY. Targeting quantum dots to surface proteins in living cells with biotin ligase. *Proc Natl Acad Sci U S A*. 2005;102:7583–7588.
37. Danjo Y, Watanabe H, Tisdale AS, et al. Alteration of mucin in human conjunctival epithelia in dry eye. *Invest Ophthalmol Vis Sci*. 1998;39:2602–2609.
38. Extrand CW, Kumagai Y. Liquid drops on an inclined plane: the relation between contact angles, drop shape, and retentive force. *J Colloid Interface Sci*. 1995;170:515–521.

Investigative Ophthalmology & Visual Science